JOURNAL OF MATERIALS SCIENCE **36** (2001) 5155–5159

The effect of stress triaxiality on tensile behavior of cavitating specimens

P. D. NICOLAOU
Silver and Baryte Ores Mining Co., S.A., 21A Amerikis Str., 106 72, Athens, Greece
E-mail: P.Nicolaou@S.andB.gr

S.L. SEMIATIN
Air Force Research Laboratory, Materials and Manufacturing Directorate, AFRL/MLLM, Wright-Patterson Air Force Base, OH 45433-7817, USA

A force-equilibrium approach was utilized to simulate the tensile behavior of sheet specimens under cavitating conditions. Unlike previous work, the current model incorporated the effect of stress state on the cavity growth rate parameter η. It was found that stress triaxiality that develops after quasistable deformation has a relatively small effect on η. Thus, at a given level of true strain, the increased value of η leads to higher cavity volume fraction inside the specimen. Simulation results revealed that tensile elongation is not affected by the higher cavity growth rate parameter when failure is localization controlled; however, in cases in which failure is fracture (cavitation) controlled, the overall elongation decreases.

1. Introduction

During uniaxial tension of a sheet specimen or round bar, plastic instability is followed by flow localization and the formation of a neck that eventually leads to failure. Bridgman [1] was the first to show that tensile hydrostatic stresses develop in the neck; such stresses tend to stabilize the deformation and enhance tensile ductility [2]. The magnitude of the hydrostatic stress is a maximum at the center of the specimen and decays to zero at its surface. The average hydrostatic stress across the section is quantitatively described by the so-called stress triaxiality factor F_T [1, 2] which depends on the neck geometry and the nature of the specimen (round bar, sheet, etc.).

During tension testing at elevated temperatures, cavitation may occur and influence the tensile behavior as well as the mode of failure. It has been shown that failure of a cavitating material may be controlled by flow localization (in which a neck is formed) *or* by fracture (essentially no neck is formed). The first mode prevails at low values of the strain rate sensitivity m and/or low cavity growth rates η_o, while the latter at large m and/or large values of η_o [3, 4].

Although stress triaxiality has a beneficial effect upon the tensile ductility when there is no cavitation, the increased stress triaxiality and hence the (tensile) hydrostatic stress may lead to an increased rate of cavity growth in cavitating materials and thus may have an adverse effect on tensile ductility. In a previous paper [4], the quantitative effects of m and η_o on the tensile behavior of materials were assessed for the case in which η_o was considered to be *independent* of the stress state. The present work was undertaken to establish the effect of stress triaxiality on tensile ductility through its influence on cavity growth. For this purpose, numerical simulations of the sheet tension test incorporating the effects of stress triaxiality on necking and cavitation were conducted and compared to previous results.

2. Modeling procedures

A numerical model based on a load-equilibrium approach was developed to determine the effect of stress triaxiality on tensile failure. The key features that distinguish the present work from that done previously [4] were the incorporation of a description of cavity growth as a function of stress state (and strain) into the previous formulation. The required modifications and calculation procedures are described in this section.

2.1. Model formulation

2.1.1. Cavity growth rate

Under most conditions of tensile deformation, cavity growth is controlled by plasticity mechanisms, and the evolution of the cavity volume fraction C_v with the true plastic strain ε is found to obey the following relation [5]:

$$C_v = C_{vo} \exp(\eta_{APP}\, \varepsilon), \tag{1}$$

In this equation, C_{vo} is a parameter used to fit experimental results and is referred to as the initial cavity volume fraction; η_{APP} denotes the average cavity growth rate parameter. The latter is also determined from experimental plots of $\ln C_v$ vs. ε.

In the present work, the cavity growth rate parameter was assumed to depend on the local stress state and, in particular, on the ratio of the hydrostatic and effective components of the local stress tensor. In this regard, the

effect of stress state on the cavity growth rate has been assessed by Rice and Tracey [6], Pilling and Ridley [7], and Budianski *et al*. [8], among others.

For the purpose of this work, the Rice and Tracey model [6] was employed in order to incorporate the influence of stress state on the cavity growth rate parameter. In particular, Rice and Tracey considered a spherical void (cavity) within a plastic, non-hardening, Mises material. The strain field was determined from three contributions: (i) a uniform strain field due to plastic deformation of the matrix, (ii) a spherically symmetric strain field resulting from the change of the void volume but no shape change, and (iii) a strain field (decaying at remote distances) which arises from changes of the void shape but not its volume. The theoretical analysis of Rice and Tracey revealed that the contribution of the change of the cavity shape in the strain field is minimal; on the other hand, the other two factors had a much more potent effect. In fact, they showed that by neglecting the cavity-shape-change strain field, the error introduced was below 1 pct.

The Rice-and-Tracey analysis led to the determination of a measure of the cavity growth rate known as the void growth factor D:

$$D = \frac{\dot{R}}{\dot{\varepsilon} R} = \frac{\mathrm{d} \ln R}{\mathrm{d}\varepsilon}. \tag{2}$$

or

$$R = R_\mathrm{o} \exp(D\varepsilon) \tag{3}$$

in which R, R_o, ε, and $\dot{\varepsilon}$ denote the instantaneous and initial void radii and the far-field strain and strain rate, respectively. The dependence of D on stress was shown to be as follows [6]:

$$D = 0.558 \sinh(3\sigma_\mathrm{M}/2\bar{\sigma}) + 0.008\ \nu \cosh(3\sigma_\mathrm{M}/2\bar{\sigma}), \tag{4}$$

in which σ_M is the hydrostatic stress; $\bar{\sigma}$ is the effective stress; and ν denotes a function of the strain rates defined as $\nu = -3\dot{\varepsilon}_2/(\dot{\varepsilon}_1 - \dot{\varepsilon}_3)$, with $\dot{\varepsilon}_1 \geq \dot{\varepsilon}_2 \geq \dot{\varepsilon}_3$ representing the principal strain rates. For example, for uniaxial stress conditions, $\sigma_\mathrm{M}/\bar{\sigma} = 1/3$, $\nu = +1.0$, thus and $D = 0.30$. For now on, the value of D for pure uniaxial conditions will be indicated as D_U. Equation 3 thus incorporates the effect of the local stress state (via D) on the growth of an individual cavity.

The void growth factor D can be used to estimate the effect of stress triaxiality on the cavity growth rate parameter. Specifically, earlier *experimental* studies concerned with cavity growth under pure tensile conditions (i.e. $\sigma_\mathrm{M}/\bar{\sigma} = 1/3$) established that the plasticity-controlled growth of an *individual* cavity obeys the following relationship:

$$R = R_\mathrm{o} \exp\left(\frac{\eta_\mathrm{o}}{3}\varepsilon\right) \tag{5}$$

in which η_o is the volumetric cavity growth rate parameter under uniaxial stress condition ($\eta_\mathrm{o} = \mathrm{d} \ln V/\mathrm{d}\varepsilon$).*

* Several analyses have led to relationships (for pure uniaxial tension conditions) between the cavity growth rate η_o and the strain rate sensitivity index of the material. For example, Stowell [9] suggested that $\eta_\mathrm{o} = 1/m$, while Cocks and Ashby [10] determined the more complicated relationship: $\eta_\mathrm{o} = 1.5(\frac{m+1}{m}) \sinh[\frac{2}{3}\frac{(2-m)}{(2+m)}]$.

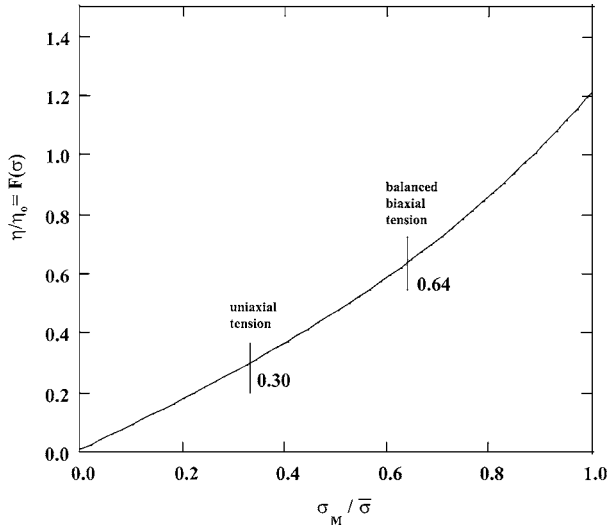

Figure 1 Dependence of η/η_o on the ratio of the mean to hydrostatic stress ($\sigma_\mathrm{M}/\bar{\sigma}$).

The cavity growth rate η_o is a parameter which also depends on the intrinsic features of a material (e.g. grain size, inclusion volume, size and spacing), as well as the deformation conditions (strain rate and temperature). Based on the analysis of Rice and Tracey, a simple relation describing the effect of stress state on the cavity growth rate can therefore be postulated. The increase of the cavity growth rate parameter η_o due to stress triaxiality is assumed to be proportional to D/D_U:

$$\eta = \eta_\mathrm{o} \frac{D}{D_U} \quad \text{or} \quad \eta = \eta_\mathrm{o} F(\sigma), \tag{6}$$

in which η denoted the cavity growth rate parameter under the complex stress state and $F(\sigma) = D/D_\mathrm{U}$. The dependence of $F(\sigma)$ on the ratio of the mean to the effective stress $\sigma_\mathrm{M}/\bar{\sigma}$ is shown in Fig. 1. $F(\sigma)$ and hence the average cavity growth rate increases as $\sigma_\mathrm{M}/\bar{\sigma}$ increases. For example, at the same strain level, the cavity size and volume fraction would be higher in the case of biaxial tension compared to uniaxial tension.

In the present work, η as defined in Equation 6 was assumed to also provide a reasonable approximation for η_APP in Equation 1.

2.1.2. Stress state at the neck

At any instant of deformation, the axial load P is given by:

$$P = A\bar{\sigma}/F_\mathrm{T} \quad \text{or} \quad \sigma_\ell^{av} = \bar{\sigma}/F_\mathrm{T}, \tag{7}$$

in which A and F_T are the local values of the cross-sectional area and the stress triaxiality factor respectively, $\bar{\sigma}$ is the effective stress, and σ_ℓ^{av} denotes the average axial stress required to sustain further deformation. Assuming that the material is plastically isotropic (i.e. the normal plastic anisotropy parameter r is equal to unity), the stress triaxiality factor F_T for a sheet

specimen is of the following form [1]:

$$F_T = \left\{ \left(1 + 2\frac{R}{a}\right)^{1/2} \ln\left[1 + \frac{a}{R}\left(\frac{2a}{R}\right)^{1/2} \times \left(1 + \frac{1}{2}\frac{a}{R}\right)^{1/2}\right] - 1 \right\}^{-1} \quad (8)$$

where a is half of the sheet width, and R the profile radius of the neck. Although strictly applicable only at the symmetry plane of the neck, Equation 8 has been shown previously [11] to give a reasonable estimate of F_T even away from the symmetry plane provided the local values of a and R are inserted into the relation.

The magnitude of the average hydrostatic stress p over the specimen cross-section, which develops after necking starts, depends on the factor F_T and the material flow stress $\bar{\sigma}$. In particular, according to the Bridgman analysis, it can be deduced that:

$$p = \bar{\sigma}\left(\frac{1}{F_T} - 1\right) \quad (9)$$

For a convex neck, $F_T < 1$ and the hydrostatic stress is tensile, while it is compressive for a concave neck in which $F_T > 1$.

The mean stress σ_M is then given by:

$$\sigma_M = \bar{\sigma}\left[\frac{1}{3} + \left(\frac{1}{F_T} - 1\right)\right]. \quad (10)$$

The ratio of the mean to the effective stress $\sigma_M/\bar{\sigma}$, which influences the temporal rate of a cavity growth, is then simply:

$$\frac{\sigma_M}{\bar{\sigma}} = \left[\frac{1}{3}\left(\frac{1}{F_T} - 1\right)\right]. \quad (11)$$

2.2. Simulation procedures

A detailed description of the simulation procedure can be found in previous publications [2, 4, 12]. However, a brief description of the input data, the numerical method, and the modifications needed to account for the effect of stress triaxiality on cavity growth is given here.

A sheet specimen geometry was considered; its gage length was assumed to be 12.5 mm and its nominal width 3.175 mm. The specimen was divided into slices (elements) which were 0.25 mm long. In all cases, a 2 pct. taper was assumed. This specimen geometry is similar to the one which has been employed to investigate the high-temperature deformation and cavitation of metallic materials [13, 14].

The material behavior was assumed to be rigid, viscoplastic, i.e.

$$\bar{\sigma} = K\left(\frac{\dot{\bar{\varepsilon}}}{\dot{\bar{\varepsilon}}_o}\right)^m \quad (12)$$

in which K is the strength parameter, $\dot{\bar{\varepsilon}}$ is the effective strain rate, and $\dot{\bar{\varepsilon}}_o$ is a reference strain rate. The initial cavity volume fraction C_{vo} was taken to be 10^{-4}.

The simulation steps were as follows:

(i) An increment of deformation was imposed and a/R and F_T were calculated for each slice.

(ii) From the F_T value, the mean and effective stresses and the cavity growth rate η, were calculated using Equations 4, 6, 10, and 11.

(iii) The true strain and strain rate distribution were calculated for each element.

(iv) From the true strain and the cavity growth rate, the increment in cavity volume fraction was determined from an equation of the form $C_{v(i)} = C_{v(i-1)} \exp(\eta_i \Delta\varepsilon)$, in which $C_{v(i)}$ is the cavity volume fraction for step i, $C_{v(i-1)}$ the cavity volume fraction for the previous step, η_i the cavity growth rate of step i, and $\Delta\varepsilon$ the true strain increment between steps $i-1$ and i.

(v) From the true strain, the cavity volume fraction, and the strain rate distribution, the new specimen dimensions, the load bearing area, the engineering stress and strain were calculated.

(vi) Steps (i) to (v) were repeated until a sharp neck was formed (localization-controlled failure) or the cavity volume fraction at the central element reached a value of 0.3 (fracture/cavitation-controlled failure). Note that extensive cavity coalescence is taking place at those levels of cavity volume fractions.

3. Results and discussion

The principal results of the present research were predictions of the effect of stress triaxiality on cavity growth, stress-strain curves, tensile elongation, and reduction in area.

3.1. Cavity growth rate vs. elongation

The evolution of the cavity growth rate of the central element η (as determined from Equation 6) normalized by the nominal cavity growth rate η_o as a function of engineering strain is shown in Fig. 2 for the case of a low strain rate sensitivity value ($m = 0.1$). In addition,

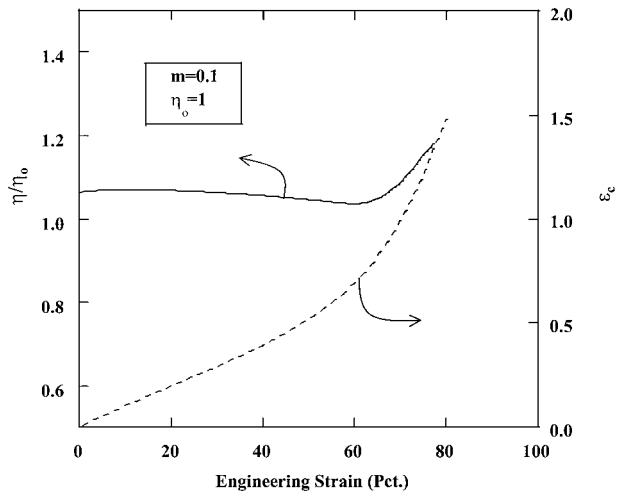

Figure 2 Model predictions for the evolution of the ratio η/η_o (solid curve) and the true strain in the central element in the tension specimen (broken line) as a function of the engineering strain for a case involving $m = 0.1$ and $\eta_o = 1$.

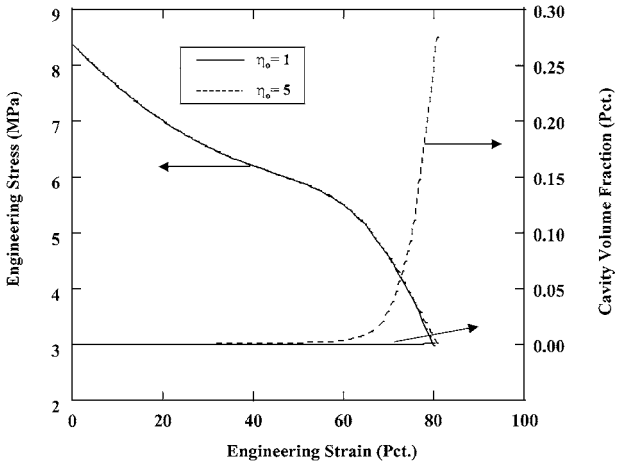

Figure 3 Simulation results for engineering stress-strain curves and cavity volume fraction vs. engineering strain for $m = 0.1$ and two different values of the nominal cavity growth rate η_o.

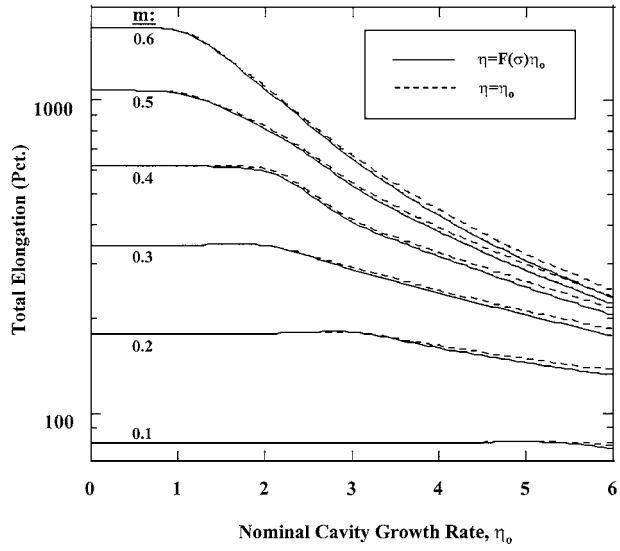

Figure 4 Model predictions of total elongation as a function of the nominal cavity growth rate η_o and the strain rate sensitivity index m for cases in which the effect of stress triaxiality on cavity growth was or was not taken into account.

the evolution of the true strain ε_c in the central element of the tension specimen is also plotted in the graph. During the quasi-stable deformation regime, the ratio η/η_o remained essentially constant and slightly above unity.† However, when necking started, the stress triaxiality effect led to a sharp increase of the cavity growth rate. As will be discussed in subsequent sections, this increase in cavity growth rate had a noticeable effect on failure behavior.

At higher values of the strain rate sensitivity, the material flow was predicted to be much more uniform, and thus η/η_o remained close to unity until very late stages of the deformation process.

3.2. Stress-strain curves

Predicted engineering stress-strain curves for a strain rate sensitivity index $m = 0.1$ and two nominal cavity growth rates η_o (1 and 5) are presented in Fig. 3. In addition, the cavity volume fraction at the central, highest-strain, element of the specimen is also shown. In both cases, failure was localization controlled. The results indicate that the presence of cavities within the specimen did not cause any changes in the stress-strain curves. This finding is in agreement with previous numerical [4] and theoretical [15] analyses.

3.3. Total elongation

As noted in the previous two sections, stress triaxiality leads to a higher-than-nominal cavity growth rate. Therefore, at a given strain (or elongation) the volume fraction of cavities would be higher. However, it was also observed that when failure is localization controlled, the engineering stress-strain behavior is affected very little when cavitation occurs. Hence, it was hypothesized that stress triaxiality would affect tensile ductility only when failure is controlled by fracture.

The dependence of the total elongation on the nominal cavity growth rate η_o and the strain rate sensitivity index m is shown in Fig. 4. The solid lines correspond to the case in which the stress triaxiality was taken into account, while the broken lines correspond to the case in which the cavity growth rate remained fixed and equal to the nominal one throughout the tension simulation. As expected, stress triaxiality was found to have no influence on total elongation when failure is localization controlled; i.e. for cases involving low values of m or η_o. On the other hand, when failure is fracture controlled, stress triaxiality was predicted to lead to a decrease in the total elongation. Moreover, the results shown in Fig. 4 indicate the transition in failure mode. In particular, for a given value of m, the transition from localization-controlled failure to fracture-controlled failure occurs at the point at which the total elongation ceases to be independent of η_o. In addition, the value of η_o at which the transition occurs decreases with increasing m.

3.4. Reduction in area

Model predictions for the reduction in area (RA) as a function of η_o and m are shown in Fig. 5. These results resemble those for the total elongation. Specifically, the reduction in area was predicted to be essentially independent of m when failure is fracture controlled. In addition, when the stress triaxiality effect is taken into account in determining the cavity growth rate, the RA is slightly lower in comparison to the results for simulations without an effect of triaxiality on η. This finding is a result of the fact that the critical cavity volume fraction for fracture ($C_v = 0.3$) is reached at lower deformations when the effect of stress triaxiality on cavity growth is taken into account.

3.5. Round bar geometry

Simulations similar to those described above were conducted for round bar specimens in order to establish the

† The fact that η/η_o is above unity is a result of the 2% taper assumed along the specimen length.

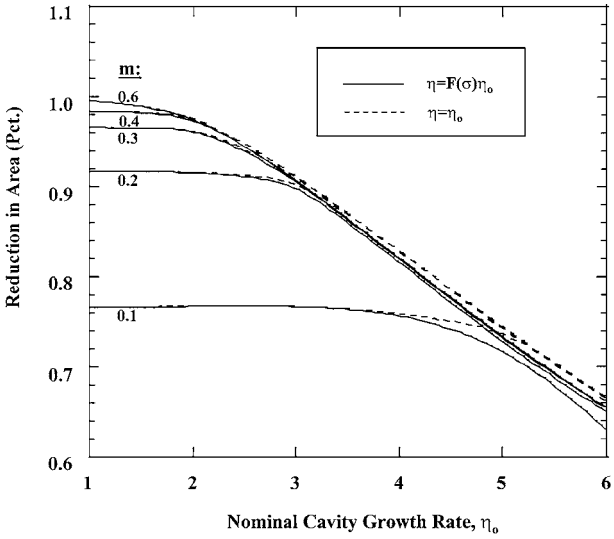

Figure 5 Model predictions of reduction in area as a function of the nominal cavity growth rate η_o and the strain rate sensitivity index m for cases in which the effect of stress triaxiality on cavity growth was or was not taken into account.

stress triaxiality effect on tensile failure for this geometry also. From a qualitative point of view, the simulation results were quite similar to those obtained for the sheet geometry. The only difference was that the incorporation of the effect of stress state on the cavity growth rate parameter had a slightly *weaker* effect on the tensile ductility. This was attributed to the fact that the factor F_T is larger for the round bar geometry compared to the sheet one for the same a/R ratio.

4. Summary

The effect of the triaxial stress state developed at the neck and its vicinity on the tensile behavior of cavitating sheet specimens was investigated using a numerical model based on a load-equilibrium approach. It was found that the stress triaxiality leads to increased cavity growth rates especially after the quasi-stable deformation regime. The increased cavity growth rate does not affect tensile behavior when failure is localization controlled despite the fact that higher cavity volume fractions are present at failure. On the other hand, when failure is fracture (cavitation) controlled, it was found that the predicted tensile elongation and the reduction in area are lower when stress triaxiality is taken into account, however its overall effect is not very large.

Acknowledgments

This work was conducted as part of the in-house research activities of the Processing Science Group in the Metals, Ceramics, & NDE Division, Air Force Research Laboratory, Materials and Manufacturing Directorate. One of the authors (PDN) was supported under the auspices of the Air Force Contract No. F33615-96-C-5251.

References

1. P. W. BRIDGMAN, in "Studies in Large Plastic Flow and Fracture" (McGraw-Hill, New York, NY, 1952) p. 36.
2. S. L. SEMIATIN, A. K. GHOSH and J. J. JONAS, *Metall. Trans. A* **16A** (1985) 2039.
3. J. LIAN and M. SUERY, *Mater. Sci. Technol.* **2** (1986) 1093.
4. P. D. NICOLAOU, S. L. SEMIATIN and C. M. LOMBARD, *Metall. Mater. Trans. A* **27A** (1996) 3112.
5. M. J. STOWELL, in "Superplastic Forming of Structural Alloys," edited by N. E. Paton and C. H. Hamilton (TMS-AIME, Warrendale, PA, USA, 1982) p. 321.
6. J. R. RICE and D. M. TRACEY, *J. Mech. Phys. Solids* **17** (1969) 201.
7. J. PILLING and N. RIDLEY, *Acta Metall.* **34** (1986) 669.
8. B. BUDIANSKI, J. W. HUTCHINSON and S. SLUTSKY, in "The Rodney Hill 60th Anniversary Volume," edited by H. G. Hopkins and M. J. Sewell (Pergamon Press, Oxford, England, 1982) p. 13.
9. M. J. STOWELL, *Metal Sci.* **14** (1980) 267.
10. A. C. F. COCKS and M. F. ASHBY, *ibid.* **16** (1982) 465.
11. C. M. LOMBARD, R. L. GOETZ and S. L. SEMIATIN, *Metall. Trans. A* **24A** (1993) 2039.
12. P. D. NICOLAOU and S. L. SEMIATIN, *Scripta Mater.* **36** (1997) 83.
13. C. M. LOMBARD, A. K. GHOSH and S. L. SEMIATIN, in "Advances in the Science and Technology of Titanium Alloy Processing," edited by I. Weiss, R. Srinivasan, P. J. Bania, D. Eylon and S. L. Semiatin (The Minerals, Metals, and Materials Society, Warrendale, PA, 1996) p. 161.
14. P. D. NICOLAOU and S. L. SEMIATIN, *Metall. Mater. Trans. A* **27A** (1996) 3675.
15. L. WEBER, M. KOUZELI, C. SAN MARCHI and A. MORTENSEN, *Scripta Mater.* **41** (1999) 549.

Received 17 October 2000
and accepted 5 July 2001